IOSR Journal of Mechanical and Civil Engineering (IOSR-JMCE)
e-ISSN: 2278-1684,p-ISSN: 2320-334X, Volume 12, Issue 2 Ver. II (Mar - Apr. 2015), PP 23-33
www.iosrjournals.org

Vibration Propulsion of a Mobile Robot

Ivan Antonov Loukanov
Department of Mechanical Engineering, University of Botswana, Botswana

Abstract: *This paper presents the original work done by the author in his effort to transform the rotating motion of two synchronized eccentric masses into rectilinear unidirectional motion of a mobile robot placed on frictional ground. Although most of the inertial drives are considered defying the laws of motion the proposed vibration propulsion is proved working without contradicting those laws. Based on this technique a wheeled robot vehicle is designed, build and successfully tested on various friction surfaces attaining a maximum towing force of 8.5 [N] while having a weight of 25 [N]. The motion is achieved by using inertial and friction forces, one-way roller bearings installed in the hub of wheels and setting an oscillating propulsion system incorporated into the robot to resonance. By altering the magnitude of the oscillating mass or the stiffness of spring system the resonance frequency of the oscillating system is changed. In order to improve furthermore the propulsion abilities of the robot it is recommended increasing the magnitude of eccentric masses and redesigning the robot in such a way a reversed motion is obtained. The suggested modifications will improve the towing and the steering ability of the robot, making it more effective in real applications.*
***Keywords** - Dean's drive, eccentric masses, inertial propulsion, one-way bearings, resonance oscillations*.

I. Introduction

There are many useful industrial application of induced vibrations caused by counter-rotating eccentric masses e.g. crashing ore, drilling rocks, separating of valuable materials in the mining and flotation industry, pumping crude oil or ground water from deep wells, etc. [1], [2], [3]. For many decades' researches and enthusiasts from all over the world have made incredible attempts to invent a device capable of defying Newton's Laws of motions by using inertia forces generated by two contra-rotating masses. So far there have been granted hundreds of patent for such devices claiming by their authors that they generate unidirectional inertial forces by converting the rotary motion of eccentric masses into linear motion such as [3, 4], and many others.

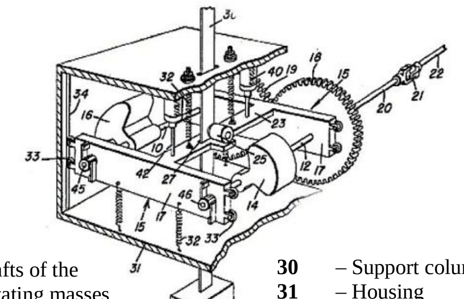

10, 12 – Shafts of the
14, 16 – Rotating masses
15, 17 – Oscillating carrier
18, 19 – Synchronizing gears
20, 22 – Input driving shaft
25 – One-way friction
30 – Support column
31 – Housing
32 – Tension springs
33, 34 – Guiding rollers & rails
40, 42 – Electro-magnetic actuators
45, 46 – Micro-electrical switches

Fig. 1 shows schematically the 3D - Dean Drive

Unfortunately most of the published patents did not work according to the expectations, others appear disappointing their inventors, but there are some small numbers of patents being exceptional in terms of their design and performance. Unfortunately these are still disputable and not accepted by the conservative scientific society. They are known as inertial propulsion engines, impulse engines, reactionless drives, inertial drives, non-linear propulsion, etc. The most fascinating invention of this type is that of N. Dean [3]. This device, commonly known as "Dean's Drive" shown in Fig 1, employs two contra-rotating eccentric masses mounted on a carrier, which in turn is guided along vertical rails and is attached to the housing by means of tension springs. According to [3] by dragging the frame of the carrier when the latter passes through its equilibrium position the drive gains a unidirectional propulsion force of nearly 5% of the weight of the mechanism. Fig. 1 illustrates schematically the Dean inertial drive as shown in his patent along with the terms of the positions labeled in the sketch. Another noticeable resent development in the inertial propulsion is proposed and profoundly studied by Provatidis [4]. This study investigates the possibility of continuous sliding propulsion of a rigid body driven also by two contra-rotating masses. The device is placed on a horizontal frictional surface and is propelled by a specially designed rotation cycle of an electric motor spinning the eccentric masses. The principle of propulsion is based upon the difference in the static and kinetic coefficient of friction between the body and the horizontal friction surface to achieve a unidirectional motion. Therefore it does not violate the Newton' laws of motion and should be treated as a reaction inertial drive.

For many years the author of this paper has designed, constructed and tested various propulsion devices employing either two contra-rotating masses as in the Dean's drive, or two synchronized pendulums, or using gyroscope-like rotating eccentric masses (Not published yet). The latter masses trace out 3D trajectories similar to figure-eight shape located on the upper halve of a spherical surface. A mechanism similar to the Dean' drive was also used in the study [5] for pumping ground water from shallow to medium-depth boreholes. Also the author has designed and built several models and prototypes of inertial pumps, being either engine, motor, or solar powered, which were successfully tested in Botswana. The study done in [6] presents a theoretical analysis of a friction dependent inertial drive also employing the Dean's drive mechanism. Although that study is greatly simplified, it shows that if the inertial drive is scaled up it may be used for driving heavy duty wheeled or caterpillar tractors operating at low speed as anticipated by Goncharevich [7].

It should be acknowledged that the author independently invented, designed and developed the proposed drive as his personal idea before seeing the Russian Patent [8], where the book [7] was quoted as an existed source. A year later the author obtained the book from a Russian library and for his surprise a similar drive was discussed on pages 173-176 with minor differences in the dynamic model of the propulsion system.

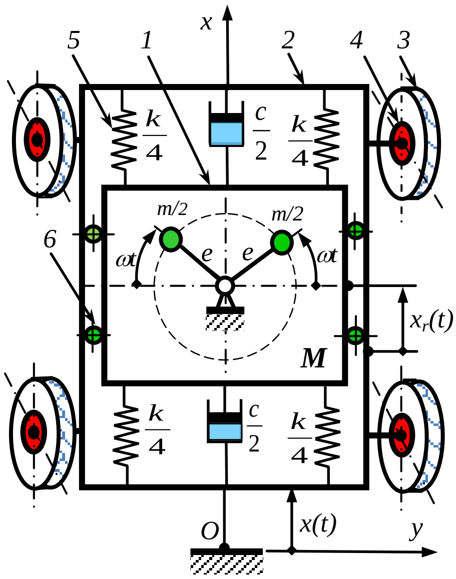

Fig. 2 shows the dynamic model of the propulsion system, where 1 is the outer frame, 2 is the inner frame carrying the oscillating system, 3 are the wheels fitted with a one-way bearing 4 allowing forward rotation and preventing the backward one, 5 is a spring from the propulsion system and 6 are linear bearings.

The current paper presents the study of one of the recently designed vibration propulsion system built into a small robot vehicle. The latter is powered by a single degree-of-freedom oscillating system excited in near-to-resonance conditions by two contra-rotating masses as it is done in the Dean's drive (Fig. 1). This system was successfully used in inertial pumps developed by the author [6], as well as in vibration drive of vehicles [7]. It should be noted that the motion of the drive is dependent upon the friction forces between the wheels and the ground thus it does not defy the Newton's laws of motion and should be considered as a friction drive. It is the author's believed that the proposed method of propulsion could be used to power specially designed robots for variety of military and industrial applications. If its power is proportionally increased it may be used as proposed in [7] but as an extra source of propulsion or in combination with the conventional gear train (torque) drives.

II. Dynamic Model and Theoretical Analysis

Considering the problems observed in most of the patents issued to date on this subject matter, a vibration propulsion system was designed, built and successfully tested. Fig. 2 show the dynamic model of the proposed propulsion drive similar to that investigated in [6] and proposed in [7]. The new design consists of two frames connected by means of tension springs and linear bearings. The inner frame (carrier) consists of an excitation mechanism composed of two counter-rotating eccentric masses synchronized by two gears (Dean Drive) and powered by a small DC motor, delivering maximum of 6 Watt power. The outer frame (chasses) carries the inner frame, the spring system, the linear ball bearings and the wheels having their axes fixed to the outer frame.

The parameters of the dynamic model of the above propulsion system are as follows:

m - total mass of rotating unbalanced eccentric masses, [kg];
e - eccentricity of rotating masses (the radius of offset), [m];
me- the unbalance of rotating masses, [kg.m]
M - total mass of the oscillating system including the mass of the inner frame and half of the mass of the linear ball bearings, [kg];
c - damping constant of the viscous damper assumed to represent the internal friction in the springs, [N.s/m];
k - stiffness of the spring elastic suspension, [N/m];
ω - angular velocity of rotating masses, [rad/s];
x_r - relative displacement between the inner & outer frames, [m];
x - absolute displacement of the outer frame, [m]
t - time, [s].

In this study a simplified engineering approach is presented when describing the propulsion system. The equation of relative motion of the oscillating system (carrier) with respect to the chasses is considered to be a single-degree-of-freedom mechanical system, although the whole propulsion system might be treated as having three-degrees-of-freedom. Consequently, it is presented in accordance with reference [9] as follows:

$$M\ddot{x}_r + c\dot{x}_r + kx_r = me\omega^2 \sin(\omega t) \tag{1}$$

The above equation is an ordinary differential equation (ODE) with constant coefficients, having a special right-hand side of the type $F(t) = F_o \sin(\omega t) = me\omega^2 \sin(\omega t)$.

The steady-state solution of the system response, signifying the resonance oscillations is determined in accordance with the type of excitation force and is given by the particular solution of (1) in the form:

$$x_r(t) = X_r \sin(\omega t - \psi)\text{, [m]} \tag{2}$$

Where: X_r is the relative resonance amplitude of inner frame with respect to the outer one, which is given by:

$$X_r = \frac{me\omega^2}{\sqrt{(k - M\omega^2)^2 + (c\omega)^2}}\text{, [m].} \tag{3}$$

The phase angle ψ in (2) is obtained from the expression:

$$\psi = \tan^{-1}\left(\frac{c\omega}{k - M\omega^2}\right)\text{, [rad]} \tag{4}$$

The latter indicates that the response of the oscillating system lags the action of the excitation force $F_o(t)$. Since the oscillating system is designed to operate in close-to-resonance conditions the phase angle ψ is always close to $\pi/2$ [rad], regardless of the amount of damping. Therefore the oscillating system responds after a delay of $\psi \approx \pi/2$ [rad] when the excitation force $F(t) = F_o \sin(\omega t)$ has been applied by the rotating eccentric masses.
By substituting (3) and (4) into (2) the resonance oscillations of the inner frame with respect to the outer one may be presented in the form:

$$x_r(t) = \frac{me\omega^2}{\sqrt{(k - M\omega^2)^2 + (c\omega)^2}} \cdot \sin\left(\omega t - \frac{\pi}{2}\right)\text{, [m]} \tag{5}$$

For a robot usage it is very important to determine the amplitude of the force transmitted from the inner to the outer frame through the springs and the inner damping. So the total force transmitted is made up of spring force and damping force components, the latter being assumed to be treated as a linear (fluid) damping:

$$\begin{aligned} F_T &= \sqrt{(kX_r)^2 + (c\omega X_r)^2} = kX_r\sqrt{1 + \left(\frac{2\varsigma\omega}{\omega_n}\right)^2} = \\ &= \frac{(F_o/k)}{\sqrt{[1-(\omega/\omega_n)^2]^2 + [2\zeta\omega/\omega_n]^2}} \cdot (k) \cdot \sqrt{1 + (2\zeta\omega/\omega_n)^2} \end{aligned}\text{, [N]} \tag{6}$$

where: $\omega_n = \sqrt{\frac{k}{M}}$ is the natural frequency of the non-damped oscillating system, [rad/s] and:

$$\varsigma = \frac{c}{2M\omega_n} = \frac{\delta}{\sqrt{4\pi^2 + \delta^2}}, \tag{7}$$

is the damping factor of the oscillating system determined through the logarithmic decrement of free vibrations:

$$\delta = \frac{1}{n} \cdot \ln\left(\frac{X_{r,(o)}}{X_{r,(n)}}\right) \tag{7a}$$

By definition the force transmissibility (*TR*) of the oscillating system to the foundation (the chasses) is defined as the ratio of the amplitudes of the transmitted force to that of the excitation force. Thus substituting (6) into that ratio eliminates the amplitude of the excitation force to get:

$$TR = \frac{F_T}{F_o} = \frac{(F_o/k)\cdot(k)\sqrt{1+(2\zeta\omega/\omega_n)^2}}{F_o\sqrt{[1-(\omega/\omega_n)^2]^2 + [2\zeta\omega/\omega_n]^2}} = \sqrt{\frac{1+(2\varsigma\omega/\omega_n)^2}{[1-(\omega/\omega_n)^2]^2 + [2\varsigma\omega/\omega_n]^2}}, \tag{8}$$

Usually when vibration insulation is the objective then the transmitted force to the foundation should be minimized and therefore the frequency ratio must be $\omega/\omega_n \geq \sqrt{2}$. This means that the oscillating system should operate to the right of the resonance point $\omega/\omega_n > 1$.

Contrary to that, in this study the idea is to increase the propulsion ability of the robot therefore it requires maximizing the force transmitted to the outer frame. Under these considerations the oscillating system should operate to the left of the resonance where $0 < \omega/\omega_n < 1$. This is very important because of the objective to utilize the amplifying effect of the resonance phenomenon as applied to the transmitted force, resonance amplitudes and the resonance accelerations. Now by using (8) and the expression for the excitation force $F(t)=F_o.\sin(\omega t)$, the force transmitted to the chasses through the spring's coils and the damping effect becomes:

$$F_T(t) = [TR \times F(t)] = \sqrt{\frac{1+(2\varsigma\omega/\omega_n)^2}{[1-(\omega/\omega_n)^2]^2 + [2\varsigma\omega/\omega_n]^2}} \cdot F_o \sin(\omega t) \tag{9}$$

It is worth mentioning that when ω increases and the oscillating system enters the resonance where $\omega/\omega_n=1$, then from (9) the expression of the transmitted force F_T simplifies to

$$F_T(t) = [TR \times F_o \sin(\omega t)] = (me\omega^2)\cdot\sqrt{\frac{1+(2\varsigma)^2}{(2\varsigma)^2}} \cdot \sin(\omega t)\cdot \tag{10}$$

The radical in (10) presents the magnification factor in resonance, showing that the amplitude of $F_T(t)$ increases significantly, but owing to the damping in the springs and in the linear ball bearings the amplitudes do not become infinitely large as the case is in the absence of damping.

By varying the speed of rotating masses one can control the magnitude of the excitation force $F_o = me\omega^2$ and therefore the amplitudes of the transmitted force, resonance velocities and resonance accelerations. Essentially, the speed of rotating masses may increase until the force transmitted during the backward action of the oscillating system does not exceed the maximum friction force between the wheels and the ground surface. This requirement will prevent the wheels from sliding during the backward action of the transmitted force and allow a proper control of the forward speed and the propulsion force of the robot vehicle. In addition to that for more accurate analysis one should also consider the grip between the wheels and the ground so the combined coefficient of friction would be larger than the static one. This would let attaining greater towing force as compared to that due to the static friction only.

According to the principle of linear momentum applied to the mass center of the whole system along the *x*-axis (Fig. 2) for one period of oscillations, one can write the following combined equation:

$$M_T(v_x - v_{o,x}) = \pm\int_0^{T/2} F_T(t)dt - F_r\int_0^{T/2} dt + F_s\int_0^{T/2} dt \tag{11}$$

where: M_T is the total mass of the vehicle including the mass of the wheels and the masses of the inner and outer frames along with their components; v_{ox} and v_x, are the initial forward and final velocities of the mass center of the robot, T is the period of one oscillation of the system, $F_T(t)$ is the variable transmitted force, $F_r=\mu_r.M_T.g$ is the rolling resistance force acting on the wheels during the forward stroke of the transmitted force and $F_s=\mu_s M_T.g$ is the static friction force acting on the wheels during the backward action of the transmitted force.

In fact for correct analysis, (11) has to be split into two equations each of them applied to the forward and backward motion of the mechanical system respectively, assuming that there is no motion in the backward direction as is written below:

$$M_T(v_x - v_{o,x}) = +\int_0^{T/2} F_T(t)dt - F_r \int_0^{T/2} dt \text{, during forward motion,} \tag{12}$$

$$M_T(0 - v_{o,x}) = -\int_0^{T/2} F_T(t)dt + F_s \int_0^{T/2} dt \text{, when there is no motion in backward direction.} \tag{13}$$

For detailed analysis it is recommended that the dynamic model of the wheel need also to be considered and analyzed, including its behavior during the backward action of the transmitted force, as well as the wheel elastic and damping properties as shown in [7], the grip with the ground and other essential details. Now, the full expression of the impulse of the transmitted force during resonance in the forward and backward oscillations corresponding to the angle of rotation of eccentric masses $\theta=\omega t \in (0, 2\pi)$ may be written as:

$$I_{F_T(t)} = \pm\int_0^T F_T(t)dt = \pm(me\omega^2)\cdot\sqrt{\frac{1+(2\varsigma)^2}{(2\varsigma)^2}}\cdot\int_0^T \sin(\omega t)\,dt \tag{14}$$

Fig. 3 shows the graphical interpretation of the impulse of $F_T = F_T(t)$ given by (14), where the period of one oscillation along with the positive and negative branches of the impulse are indicated. It is obvious that the resultant impulse of the transmitted force per cycle of oscillation is zero because of the equal positive and negative branches of the impulse. Therefore according to (12) there will be no change in the linear momentum and hence there will be no unidirectional motion of the system. In this case, if the wheels are free to rotate in both directions about their axes, the action of the transmitted force will result in a forward and backward motion of the mass center of the system consistent with the positive and negative twigs of the impulses respectively.

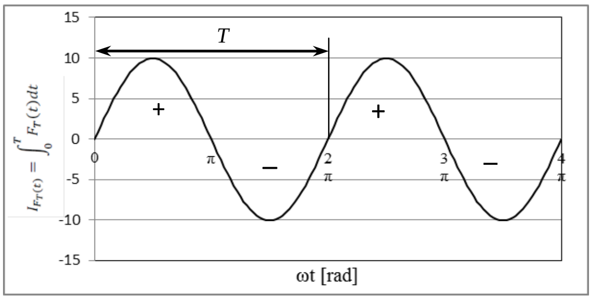

Fig. 3 displays the full impulse of the transmitted force $F_T(t)$, [N.s]

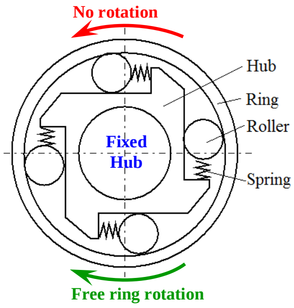

Fig. 4 shows the schematic of one-way roller bearing

Apparently this is not what is desired, so to avoid this reciprocating motion it is decided the wheels to be fitted with one-way roller bearings, also known as unidirectional mechanical clutches as suggested in [7]. The latter allowed rotation in one direction and prevents rotation in the opposite direction. Fig. 4 shows the schematically view of a one-way roller bearing. It consists of a stationary shaft and slotted hub in which rollers and springs are accommodated and one-way rotating outer ring is positioned. The actual bearings used in this study have rollers which not only achieve one-way rotation but also bear the radial loads acting upon the wheels.

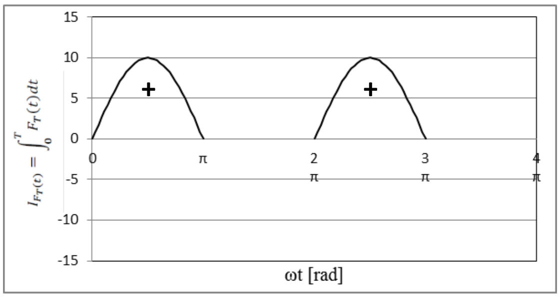

Fig. 5 indicates the remaining positive impulses of the transmitted force $F_T(t)$, [N.s]

Owing to the installation of the one-way bearings the negative impulses were removed and the positive ones remain, consequently the graph of the impulse of $F_T(t)$ changes to that as shown by Fig. 5. The remaining positive impulses change the linear momentum in *x*-direction as per (12) and a unidirectional pulsing motion of the robot vehicle is obtained. By increasing the speed of rotation of eccentric masses the frequency changes and the amplitude of excitation force $F_o = me\omega^2$ increases forcing the motion to become smoother and stronger. This pushes the oscillating system to enter the resonance zone in the ascending branch of the resonance graph where $\omega/\omega_n \rightarrow 1$ resulting in increasing the magnitude of the transmitted force. As a result the demand for a stronger friction force on the wheels during backward action of the transmitted force also increases until the maximum friction force is reached. If exceeded this eventually may cause slight slippage of the wheel in the backward direction, which is undesirable effect, as this will reduce the propulsion capacity of the robot vehicle.

III. Wheels Interaction with The Ground

The pictorial view of the prototype model vehicle and the force gauge used to measure towing forces are presented in Fig. 6. It is obvious that the axes of the wheels are fastened tightly to the outer frame and there are no hidden transmission elements rotating the wheels. As a result the propulsion of vehicle is due to the positive impulses of the transmitted force, because of the one-way bearings and the friction reactions provided by the ground upon the wheels.

The following are the parameters of the prototype robot: m = 2×0.06 kg = 0.12 [kg] is the combined mass of rotating masses fixed to the synchronizing gears at eccentricity e = 12.5 [mm]; M = 1.0 [kg] is the total mass of the oscillating system including that of rotating masses, the mass of the inner frame, synchronizing gears, the DC motor and the upper half of the mass of linear bearings; $M_{o.f.}$=1.5 [kg] is the mass of the outer frame (*o.f.*) including the mass of the wheels, the fixed shafts and the one-way bearings; M_T=2.5 [kg] is the total mass of the robot vehicle. In this design the total spring stiffness, k of the oscillating (propulsion) system may be varied when using springs of different stiffness to achieve resonance within the range of operation of the motor speed. In addition to the above parameters the mass of the oscillating system M can also be increased to study the increasing effect of the oscillating mass on the towing capacity and forward velocity of the robot vehicle.

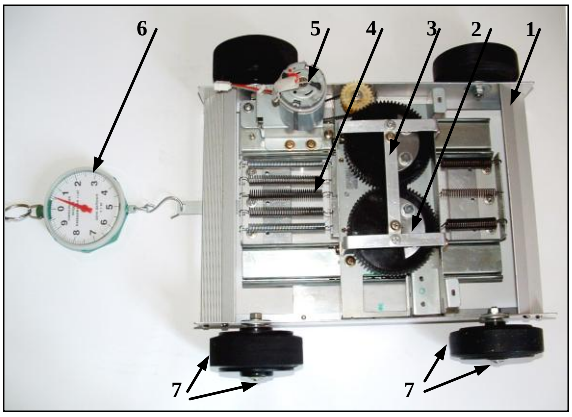

Fig. 6 shows the top view of the prototype robot vehicle, where: 1 is the outer frame, 2 - contra-rotating eccentric masses, 3 - inner frame, 4 - spring system, 5 - DC motor, 6 - the force gauge, 7 – and the wheels fitted out with one-way roller bearings.

The conducted preliminary experiments with the robot vehicle indicated that a unidirectional forward motion is achieved although in a pulsing manner, corresponding to the style of the positive impulses of the transmitted force $F_T(t)$, as seen in Fig. 5. The frequency of excitation is dependent upon of the preset resonance frequency of the system and is controlled by increasing the motor speed. The higher the natural frequency of the system the smoother the motion of the vehicle is.

In the course of conducted experiments a maximum propulsion force of 8.5 [N] is measured, depending upon the coefficient of static friction between the wheels and the contacting surface, the mass of the oscillating system, the combined mass of the eccentric masses, the frequency of oscillations and the total mass of the robot vehicle. The latter contributed to the resultant friction force as it is reliant on the normal reactions on the wheels, while the combined mass of rotating masses - m and the mass of the oscillating system - M affect the magnitude of the transmitted force as per equations (6) and (10). It is also found that in close to resonance conditions when $\omega/\omega_n \rightarrow 1$ the transmitted force attains its maximum value corresponding to the maximum forward speed and the maximum towing force developed by the robot. As long as the value of the transmitted force during its backward action does not exceed the magnitude of the static friction force between the wheels and the ground there is a robust unidirectional motion. When the vehicle is moving in a forward direction it overcomes the rolling friction force only, which is known to be much smaller than the static one. This difference helps achieving easy propulsion on soft, sandy or unstable surfaces. That depends upon the grip capacity of the wheels, the area of contact, the type of ground and the contacting pressure on the surface. Certainly these are the same parameters generally required to accomplish motion on soft and unstable soils for the conventional vehicles.

To understand how the vibration driven vehicle propels as compared to the torque driven one both methods of propulsion are further investigated and analyzed. Fig. 7 illustrates the free-body-diagram (FBD) of a torque-driven wheel of a conventional motor vehicle interacting with a frictional surface. Accordingly during uniform motion the force pushing the wheel in the forward direction is the friction force, which is balancing the toque through the wheel effective radius. When the torque $T=r_e.F_s$ increases then the static friction force F_s provided by the contact surface also increases, until the maximum friction force $F_{max}=\mu_s M_T g$ is attained. Any additional demand for friction force larger than the maximum one leads towards slippage of the wheel against the surface. Usually just before slipping occurs it is said that there is an impending slipping and any further increase of the toque will force the wheel to start sliding continuously on the surface. Thus the traction will be greatly reduced and the vehicle cannot propel itself any more. Under these conditions the traction capacity of the wheel is exceeded and the forward motion of the vehicle is seized, because of the lost grip. This is the limiting situation, which frequently occurs on rainy (wet), sandy, mud-covered or icy surfaces. When the torque driven wheels of a vehicle start slipping they penetrate deeper and dipper into the surface and the vehicle is getting trapped in ditches formed under the slipping wheels.

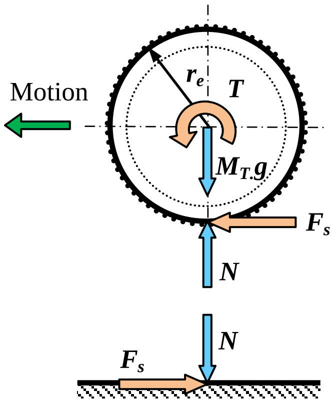

Fig. 7 shows the FBD of a torque driven wheel

Fig. 8 presents the *FBD* of a wheel driven by a variable force as per the proposed method, where the driving force is the force transmitted $\boldsymbol{F_T(t)}$ to the wheel axle via the outer frame. The effect of this force is pushing the wheel along the surface and a small amount of this force is balanced by the rolling resistance force F_r as shown in Fig. 8 (a). There are two components acting at the point of contact ***A***, where $F_r=\mu_r.N$ is the rolling resistance force and N is the normal reaction of the ground. As seen from this figure when the transmitted force acts in the forward direction then the wheel simply rolls overhead the surface and overcomes the rolling resistance force F_r only. Under these conditions the wheel is accelerated since the driving force $F_T(t)$ is much bigger than the rolling resistance forces. It should be noted that wheel accomplishes general plane motion and the point **A** acts as an Instantaneous Center of Rotation (ICR) for the wheel, since there is no slippage and the velocity of this point is zero. Therefore there are two unknown forces – N and F_r, and the kinematics parameters - a_c, ε and μ_r.

Employing the differential equations of the general plane motion for the wheels and the kinematic velocity relations to the ICR one can write:

$$
\begin{aligned}
&M_T\ddot{x}_C = F_T(t) - F_r && (a)\\
&M_T\ddot{y}_C = N - M_T\mathrm{g} && (b)\\
&I_C\ddot{\theta} = F_r r_e && (c)\\
&\ddot{y}_C = 0, \quad \text{No motion in y direction} && (d)\\
&\ddot{x}_C = a_C = r_e\,\ddot{\theta} = r_e\,\varepsilon && (e)\\
&V_C = r_e\dot{\theta} = r_e\omega && (f)\\
&F_r = \mu_r N && (g)
\end{aligned}
\qquad (15)
$$

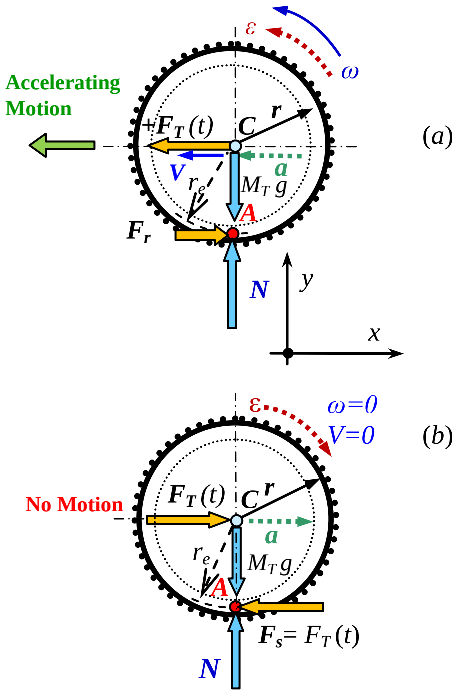

Fig. 8 displays the FBD's of a wheel propelled by a variable force $F_T(t)$ as per the proposed method, where Figs. 8(*a*) show forces during forward action and Fig. 8(*b*) during the backward action *of* $F_T(t)$.

In the above equations the effect of the impact taking place at the instant of blocking the wheels by the one-way rotating bearings during the backward action of the transmitted force is not taken into consideration. Contrary to the case presented in Fig. 7 there is no slippage or impending slipping in the analysis for the coefficient of rolling resistance, provided that the acting force F_T is constant. Then from static equilibrium of the wheel the following expression for the static coefficient of rolling resistance is determined:

$$\mu_r = \frac{F_T(t)}{M_T.g} = \frac{1}{M_T.g} \cdot (me\omega^2) \cdot \sqrt{\frac{1+4\varsigma^2}{4\varsigma^2}} \cdot |\sin(\omega t)| \qquad (16)$$

The above results suggest that the coefficient μ_r changes according to the variation of the transmitted force $F_T(t)$ when it acts in the forward direction but does not account for the wheel mass, inertia and its geometry.
In fact the transmitted force is a fluctuating as specified by (10) hence the differential equations describing the general plane motion (15) of the wheel have to be considered in determining the unknown parameters, $\ddot{x}_C = a_C$, $\ddot{\theta} = \varepsilon$, F_r, N and μ_r. The results obtained are as follows:

$$\begin{aligned}
&\ddot{x}_C = a_C = \frac{2me\omega^2\beta}{(2M_T + m_w)} \cdot \sin(\omega t), && [\mathrm{m/s^2}] \\
&N = M_T.g\,, && [\mathrm{N}] \\
&F_r = \frac{m_w}{2M_T + m_w} \cdot (me\omega^2)\beta.|\sin(\omega t)|, && [\mathrm{N}] \\
&\varepsilon = \ddot{\theta} = \frac{\ddot{x}_C}{r_e} = \frac{2me\omega^2\beta}{(2M_T + m_w).r_e} \cdot \sin(\omega t), && [\mathrm{rad/s^2}] \\
&\mu_r = \frac{F_r}{N} = \frac{1}{M_T.g} \cdot \frac{m_w}{(2M_T + m_w)} \cdot (me\omega^2)\beta.|\sin(\omega t)|, && [\text{dimensionless}]
\end{aligned} \quad , \qquad (17)$$

where the expression $\beta = \sqrt{\frac{1+(2\varsigma)^2}{(2\varsigma)^2}}$ is the dimensionless magnification factor in resonance of the system.

All the above results, with the exception of N, a_c and ε nullify when $\sin(\omega t) < 0$, because when the transmitted force $F_T(t)$ is acting in the backward direction (Fig. 8*b*), the one-way bearing prevents the wheel from rolling in this direction and therefore there will be no motion. During this time interval ($T/2$) the impulse of the transmitted force is balanced by the impulse of the static friction force F_s emanating from the ground and acting upon the wheel. When $F_T(t)$ increases then the friction force also increases until $F_s=F_{s,max}=\mu_s N$ is attained. Since the proposed propulsion is created by a variable force, this may eventually reduce the static coefficient of friction to the kinetic one - μ_k if the propulsion force becomes greater than $F_{s,max}$. This effect will ultimately decrease the towing ability of the mobile robot depending upon the difference in the coefficients of friction. On the other hand the contemporary wheels are made up of pneumatic rubber tires having special tread profile on the rim, which provides stronger grip with the ground achieved on a relatively large area of contact since they deform more than solid wheels. Also the rubber material itself offers significant vibration damping as well as strong elasticity, which both ultimately help reducing the decreasing effect of oscillations on the friction. In addition to that pneumatic tires may work as potential energy accumulators during the backward stroke of the transmitted force. Later at the beginning of the next forward stroke of the force $F_T(t)$, the accumulated energy may be added to the forward motion of the vehicle. To achieve that effect a special synchronization is required between the oscillating bodies as suggested by [7] and [10]. In summary the properties of the modern pneumatic tires offer a stable less oscillatory motion and may utilize effectively both the positive and negative impulses of the transmitted force, hence attaining better efficiency and forward speed of the robot vehicle.

Following the above analysis it may be concluded that the maximum friction force between the wheels and the ground appears to be the limiting factor to both propulsion systems; the conventional torque operated and the proposed one dependent on the inertial and friction forces. In fact the reduced coefficient of friction from static to the kinetic one will not affect significantly the forwards motion of the vehicle, hence keeping it moving. The reason is that the kinetic friction force still provides a backward support for the wheels and so the new propulsion system will not suffer of wheel slipping being blocked in a trench as in the torque driven propulsion system and therefore will not be stuck when this phenomenon occurs.

Obviously there are always advantages and disadvantages when analyzing these systems. The advantages of the new propulsion system are that it does not allow the vehicle to get trapped in trenches when moving on soft and unstable off-roads, since there are no torques acting on the wheels, hence no conventional slippage may occur. The major benefit is that the system does not require any complex transmission devices such as conventional manual or automatic gear trains, friction or hydraulic clutches, differentials, prop shafts etc. Avoiding the use of all these complex and expensive devices will contribute towards a significant reduction in the production and maintenance cost of these vehicles. Thus the above advantages make the new propulsion system useful for many military and industrial applications where the use of robot vehicles is unavoidable.

From the disadvantages of the new propulsion system apart from the low speed it is important to mention the unnecessary vibrations transmitted to the chassis (outer frame). However they can be reduced considerably by being converted into useful propulsion by considering more-degrees-of-freedom of the oscillating system and using pneumatic wheels. Also they can be hampered by employing an active vibration protection system as suggested by [11]. As a new propulsion system the proposed one may safer of some other disadvantages, but the reader should understand that the contemporary vehicles were developed and improved during the past 130 years when thousands of engineers, technicians and inventors contributed to these achievements. Accordingly one should be open-minded to the new propulsion system until it is employed in real applications and proves to be appropriate. On the other hand the designers, engineers and technicians should be given the chance to increase the performance, reliability and efficiency of this system by changing the excessive vibrations into useful propulsion or by using special techniques to reduce the unwanted residual vibrations.

IV. Experimental Analysis of the Robot Vehicle

A number of experiments were conducted with the robot vehicle, mainly on three types of surfaces: PV-tiles, important for in pipe inspection robots, Tarmac (asphalt) and Cemented (paved) both for industrial and military applications. It should be noted that the wheels used in the prototype robot vehicle are made of hard rubber, they are non-pneumatic, and their surfaces are machined thus having no thread on the rim at all. This situation resembles the state of completely warn over-pressurized tiers, which is the poorest case in the transportation practice. The towing forces were measured by using spring dynamometer furnished with additional low stiffness high damping spring-like rubber material connected in series to avoid resonance vibrations of the gauge pointer. To achieve varieties of resonance frequencies of the excitation system within the range of the motor speed up to 10 tension springs of different stiffness were used as well as three masses were added consecutively to the oscillating system. The resonance frequencies are measured by using a stroboscopic speedo-meter Helios 5003, having a range 250 - 18000 rev/min, manufactured by Branime Manufacturing Ltd, UK. The frequencies for each resonance conditions were measured in rev/min and converted into a number of oscillations per second, [Hz]. Every experiment is repeated three times and the average results are displayed in Table 1, along with the corresponding resonance frequencies. In addition to these parameters the mass ratios

M/M_T are also shown on the aforesaid experiments. In Table 1 M_T signifies the total mass of the prototype robot vehicle made up of the mass M of the oscillating system (inner frame), the mass $M_{o.f.}$ of the chasses (outer frame) and the mass m_w of the wheels.

It should be noted that measuring the resonance frequencies by using a speed tachometer may not be accurate enough and in the future it is recommended using more sophisticated means in identifying the parameters of the propulsion system. All the masses including the rotating masses where measured using an electronic scale type SKWD A1 manufactured by MGG Electro GmbH, Germany, having an accuracy of 1 [gr].

It is evident from the table that the highest traction force of 8.5 [N] is obtained on paved (cemented) surface at frequency of 13.7 [Hz]. Obviously this is due to the higher coefficient of friction offered by the surface and the wheels, the higher resonance frequency of the excitation system and the appropriate mass ratio.

Table 1 Towing forces, resonance frequencies and type of surfaces.

Type of surface material	Masses, [kg] Mass ratios	Frequencies – f, [Hz]			
Polyvinyl (PV) surface	M=1.00 M_T=2.50 M/M_T=0.4	6.33	10.7	10.8	12.5
		Towing Force – F, [N]			
		2.5	4.5	5.0	4.8
Tarmac (asphalt)	M=1.6 M_T=3.12 M/M_T=0.52	Avg. 7.5 [N] at 10.8 [Hz] Avg. 8.0 [N] at 12.5 [Hz]			
Paved (cemented)		Avg. 8.5 [N] at 13.7 [Hz]			

Following the trend of variation of the towing force it is obvious that the force increases as the frequency and the mass ratio increased. In this case the high frequencies contribute to both the increased number of positive impulses per unit of time and to the increased magnitudes of these impulses due to the amplifying effect of the resonance. On the other hand the increased mass of the oscillating system provides also enhanced transmitted force to the outer frame due to the increased normal reactions on the wheels. The latter increases the static friction force whenever the backstroke of the transmitted force takes place, hence increasing the towing force. Similar effect is observed when the total mass is increased. In case when a backward slip occurs then the static friction force becomes the kinetic one. Therefore the kinetic friction forces appears to be the limiting factors of the towing force of the robot since it hampers the grip with the ground. However, the difference between the coefficients of friction is not that much so that the robot vehicle does not losses the motion at all, contrary to the conventional torque driven wheels when experiencing a slip they are simply losing the grip and getting trapped in the trenches formed under the wheels, hence no forward motion.

V. Discussion and Conclusions

This paper presents the theoretical and experimental analysis of a vibration propulsion drive for robot vehicles operating on frictional grounds. Although the new system uses the propulsion effect of inertial forces in close-to-resonance conditions it does not defy the Newton's laws of motion and the conservation of momentum. The reason is that the propulsion is based on the static and kinetic friction forces between the wheels and the ground, similar to any other vehicle known today. The motion is achieved by eliminating either the positive or negative impulses of the transmitted force and using the propulsion effect of the remaining impulses. The latter changes the linear momentum of the mechanical system, allowing either forward or backward motion.

The experimental results obtained with a model prototype robot vehicle revealed that a maximum towing force of up to 8.5 [N] was measured on cemented surface under dry conditions. The ratio of the maximum towing force to the weight of the model vehicle is estimated to vary from 0.20 at low frequencies to 0.34 at high frequencies, not taking into consideration the grip between the wheels and the surface in contact. Because of the simplicity of the proposed design it is evident that the motion of such a vehicle does not require any complex transmission devices such as conventional friction or hydraulic clutches manual or automatic gear trains, prop-shafts, differentials, etc. The absence of the said devices makes the vibration propulsion system simple and cheap in production and easy maintained in practice. Apart of these benefits the wheels of the robot vehicle interact with the ground differently than the wheels driven by torques as the case is with conventional vehicles. This allows the new propulsion system to be used on soft and unstable surfaces where conventional drives are propelled with lots of problems. They require a four-wheel drives or even using special electronically controlled propulsion system that supply the driving wheels with suitable torques to avoid slippage. Today modern vehicles use special winter tires having improved grip with snowy-roads and also chains or metal spikes when used on icy surfaces. The latter approach may also be employed to the new propulsion system improving the grip with the ground and preventing the backward slip during the reversed stroke of the transmitted force. As long as this force is smaller than the kinetic friction force between the wheels and the ground, there will be no slippage and the motion of the robot will be achieved like pushing the vehicle with a pulsing force.

In the proposed propulsion system all the wheels provide the necessary support but only the forward stroke of the transmitted force is utilized, which constitute smaller than 50% of energy usage. To fully utilize the propulsion effect of the force $F_T(t)$, it is recommended storing the kinetic energy of the negative impulse into a potential energy in a system of springs attached between the outer frame and the axes of the wheels. When the next forward stroke of the same force takes place the potential energy stored in the springs might be converted into a kinetic energy and added to the forward motion. Therefore a combine effect of more than 75% of the towing force may be obtained. However the proposed arrangement would increase the requirement for the degrees of freedom of the oscillating system by converting the mass of the outer frame (chassis) into another oscillating body [7, 8, 9]. Apart of the above the proposed modification of the propulsion system would require an appropriate synchronization between the motions of the oscillating masses in order to achieve propulsion with an increased velocity and towing force for the same input power as specified by [10]. In addition to the proposed arrangements it is possible to change the design in a way to achieve either forward or reversed motion, thus improving the steering of the device. Also a combined torque-vibration propulsion drive could also be designed therefore combining the advantages of both propulsion systems [7]. The suggested changes will be developed and investigated after subsequent design modifications. Proper analyses will be carried out and a selection of the most appropriate design providing better efficiency would be carried out.

Possible fields of application of the proposed vibration drive is to be employed in the propulsion of small robots moving on friction surfaces and intended for an inspection of weldment and corrosion status of pipes transporting gas or liquids as well as examining and cleaning ventilation and air conditioning conduits systems in industry [11, 12]. Similarly, in order to increase safety, the propulsion device may be also used as a remotely controlled robot for examining mining tunnels, channels and shafts for the existence of Methane, CO_2 and other harmful or engine exhaust fumes before being handed over to mineworkers for further operation. The proposed driving system may be used in special military activities like a mini robots intended to identify and destroy land mines or in searching for enemy activities on the ground when equipped with video cameras. It may be also used for propelling small video-robots in underground tunnels and animal shelters for scientific studies or real time video observations.

Other possible areas of applications of the new propulsion system may be in wheeled or caterpillar earthmovers, where the low speed is not a concern but the traction capacity is important [6, 7, 8, 11]. Of course the use of the vibration propulsion system would require an appropriate increase of the power output to correspond to the intended application. For these machineries the imposed vibrations will help decreasing considerably the friction forces between the soil and the digging implement therefore reducing the traction forces required and achieving easy soil excavation and transportation.

In conclusion it is advisable that further design modifications to be undertaken so as to achieve reversible motion as well as improving the dynamic model and carrying out a precise identification of the parameters of the mechanical system. These will certainly provide better knowledge of the vibration propulsion system and make it acting better during applications in practice.

References

[1]. A. G. Bodine, Deep Well Pump, US Patent # 2, 553, 543, granted 1951.

[2]. V. M. Usakovskii, Inertial pumps (Machine-Building Publishing, Moscow, 1973, in Russian).

[3]. N. L. Dean, System for Converting Rotary Motion into Unidirectional Motion, US Patent # 2,886,976, granted 1959.

[4]. C. G. Provatidies. Design of a Propulsion Cycle for Endless Sliding on Friction Ground using Rotating Masses. Universal Journal of Mechanical Engineering, Vol. 2 (2), 2014, pp. 35-43, also available on (http:/www.hrpub.org).

[5]. I. A. Loukanov, Investigating the Pumping Process of a Resonance Vibrating Pump for Medium - depth Boreholes, Research in Agricultural Engineering 53(4), 2007, pp. 172-181.

[6]. I. A. Loukanov, Using Inertial Forces as a Source of Forward Motion, Mechanics of Machines, Vol. 110, (2), 2015, pp. 104-107.

[7]. I. F. Goncharevich, Vibration-nonstandard Approach: vibrations in nature & engineering. (Nauka, 1986, Moscow, in Russian).

[8]. A. A. Cherepanov 1996. Inertial propulsion of vehicle, Russian Patent # 2066398.

[9]. Singiresu S. Rao, Mechanical Vibrations, SI Ed. (Pearson, Prentice Hall, Singapore, 2005).

[10]. I. I. Blekhman, Synchronization in Science & Technology, (ASME Press, NY, 1988).

[11]. F.L. Chernousko. About the motion of a body containing internal moving mass. // Conference Papers published by Russian Academy of Science, Vol. 405, №1, 2005, p. 1-5 (in Russian).

[12]. Jatsun S., Jatsun S., Vorontsov R. Dynamics of vibrating robot for in pipe inspection, International Symposium – SYROM. – Bucharest, 2001, pp. 205-209.